ELSEVIER

European Journal of Pharmacology 321 (1997) 285–293

ejp

Preclinical evaluation of [^{123}I]R93274 as a SPECT radiotracer for imaging 5-HT$_{2A}$ receptors

Anissa Abi-Dargham [a,*], Yolanda Zea-Ponce [a], Dirk Terriere [b], Mohamed Al-Tikriti [a], Ronald M. Baldwin [a], Paul Hoffer [a], Dennis Charney [a], Josée E. Leysen [c], Marc Laruelle [a], John Mertens [b], Robert B. Innis [a]

[a] *Yale University School of Medicine / VA Medical Center, West Haven, CT, USA*
[b] *VUB-Cyclotron, Brussels, Belgium*
[c] *Janssen Research Foundation, Beerse, Belgium*

Received 22 October 1996; revised 11 November 1996; accepted 12 November 1996

Abstract

Studies in rodents have suggested that the radioiodinated 5-HT$_{2A}$ receptor antagonist [^{123}I]R93274 (123-iodine-*N*-[(3-*p*-fluorophenyl-1-propyl)-4-methyl-4-piperidinyl]-4-amino-5-iodo-2-methoxybenzamide) ($K_d = 0.1$ nM) might be a promising single photon emission computerized tomography (SPECT) radiotracer to image 5-HT$_{2A}$ receptors in the living human brain. In this study, we characterized the brain uptake of [^{123}I]R93274 in baboons. Highest brain uptake was observed in cortical areas, while lower uptake was observed in the striatum and the cerebellum. Injection of pharmacological doses of the 5-HT$_{2A}$ receptor antagonist ketanserin resulted in reduction of cortical and striatal radioactivities to the level observed in the cerebellum. Injection of the selective dopamine D$_2$ receptor antagonist raclopride did not affect [^{123}I]R93274 brain uptake. Quantification of 5-HT$_{2A}$ receptors was achieved by measuring the binding potential of 5-HT$_{2A}$ receptors for [^{123}I]R93274 (the binding potential is the product of the density and affinity of available receptors). Regional binding potential values were derived with a three-compartmental kinetic analysis of the time-activity curves in the brain and plasma. Binding potential values of 93 ± 34 ml/g, 71 ± 35 ml/g and 31 ± 11 ml/g were measured in the occipital, temporal and striatal regions, respectively. Similar values were derived using a noncompartmental graphical analysis. These values were in accordance with the in vitro regional distribution of 5-HT$_{2A}$ receptors in primate brain. In conclusion, [^{123}I]R93274 allows visualization and quantification of 5-HT$_{2A}$ receptors in the baboon brain with SPECT.

Keywords: 5-HT$_{2A}$ receptor; SPECT (single photon emission computerized tomography); [^{123}I]R93274

1. Introduction

Alterations of 5-HT$_{2A}$ receptors have been reported in several neuropsychiatric conditions, including depression (Stanley and Mann, 1983; Mann et al., 1986; McKeith et al., 1987; Cheetham et al., 1988; Arora and Meltzer, 1989; Gross-Isseroff et al., 1990; Yates et al., 1990; Lowther et al., 1994), schizophrenia (Bennett et al., 1979; Whitaker et al., 1981; Mita et al., 1986; Arora and Meltzer, 1991; Joyce et al., 1993; Laruelle et al., 1993) and Alzheimer's disease (Crow et al., 1984; Perry et al., 1984; Reynolds et al., 1984; Blin et al., 1993). In addition, 5-HT$_{2A}$ receptor agonism is implicated in the psychotogenic effects of hallucinogens such as *d*-lysergic acid diethylamide and the methoxyphenylisopropylamines (Aghajanian, 1994). On the other hand, 5-HT$_{2A}$ receptor antagonism is believed to play a major role in the antipsychotic activity of several atypical neuroleptics such as clozapine (Meltzer, 1989) and risperidone (Leysen et al., 1994), in particular with regard to the treatment of negative symptoms. Therefore, the ability to image and quantify 5-HT$_{2A}$ receptors in the living human brain may be useful to elucidate the pathophysiology of these conditions.

Several positron emission tomography (PET) radiotracers have been developed as probes for the 5-HT$_{2A}$ receptors, such as [^{11}C]ketanserin (Berridge et al., 1983), *N*1-([^{11}C]-methyl)-2-Br-LSD (Wong et al., 1987),

* Corresponding author. Present address: Brain Imaging Division, Department of Psychiatry, Columbia University College of Physicians and Surgeons, New York State Psychiatric Institute, Unit 28, 722 West 168th Street, New York, NY 10032, USA.

0014-2999/97/$17.00
PII S0014-2999(96)00906-5

[^{18}F]setoperone (Blin et al., 1988), [^{18}F]fluoroethylketanserin (Moerlein and Perlmutter, 1991) and [^{18}F]altaneserin (Lemaire et al., 1991). In addition, spiperone derivatives such as (3-*N*-[^{11}C]methyl)spiperone ([^{11}C]NMSP) have been used to label 5-HT$_{2A}$ receptors in cortex (Wong et al., 1984; Mayberg et al., 1988; Nyberg et al., 1993). In contrast, no tracers are currently available for imaging of 5-HT$_{2A}$ receptors with single photon emission computerized tomography (SPECT). Given the lower cost and wider availability of SPECT technology, the development of a 5-HT$_{2A}$ receptor SPECT radiotracer is warranted.

R93274, or 5-I-R91150 (*N*-[(3-*p*-fluorophenyl-1-propyl)-4-methyl-4-piperidinyl]-4-amino-5-iodo-2-methoxybenzamide) is a selective iodinated 5-HT$_{2A}$ antagonist with high affinity ($K_d = 0.11$ nM) and selectivity for 5-HT$_{2A}$ receptors (Leysen et al., in preparation; Mertens et al., 1995). The selectivity of [^{125}I]R93274 for 5-HT$_{2A}$ receptors with regard to other neurotransmitter receptors such as other 5-HT receptors (including 5-HT$_{2C}$), dopamine receptors, adrenaceptors and histamine receptors is at least a factor of 50 (Mertens et al., 1995). In vivo uptake of [^{125}I]R93274 in the brain has been studied in rodents (Mertens et al., 1995). In these studies, the radioactivity concentrated in cortical regions, with frontal to cerebellar ratios of 10 at 3 h post injection, and was displaceable with ketanserin. These data suggested that [^{123}I]R93274 might be a promising tracer to image 5-HT$_{2A}$ receptors in the human brain. In this study, we characterized the brain radioactivity uptake of [^{123}I]R93274 in baboons.

2. Materials and methods

2.1. Radiolabeling

The precursor, *N*-[(3-*p*-fluorophenyl-1-propyl)-4-methyl-4-piperidinyl]-4-amino-2-methoxybenzamide (**1**, R91150) and the 5-iodo-derivative (R93274) are original products of the Janssen Research Foundation (Beerse, Belgium). Samples of the precursor and the cold standard *N*-[(3-*p*-fluorophenyl-1-propyl)-4-methyl-4-piperidinyl]-4-amino-5-iodo-2-methoxybenzamide (**2**, R93274) were obtained from Janssen Pharmaceutica (Beerse, Belgium) (Fig. 1).

Iodination 'kits' were prepared by dispensing 50 μl (50 μg) each of a 1 mg/ml chloroform solution of the precursor (**1**) into 1 ml conical vials, evaporating the solvent to dryness with a stream of N_2, and capping with 13 mm Teflon-lined stoppers. Vials were stored at 4°C protected from light. No-carrier-added [^{123}I]NaI in 0.1 M NaOH (radionuclidic purity > 99.8%) was obtained from Nordion International (Vancouver, British Columbia, Canada). Peracetic acid (32% (w/v) solution in dilute acetic acid) was obtained from Aldrich (St. Louis, MO, USA) and diluted with sterile water just before use. All other chemicals were

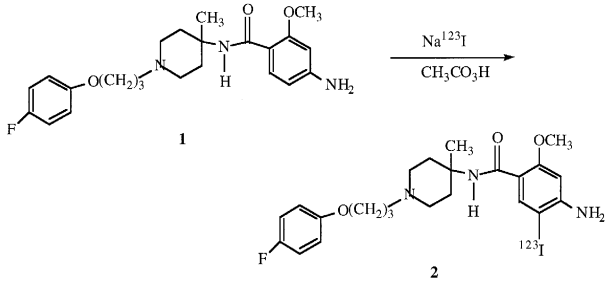

Fig. 1. Chemical structure and iodination of [^{123}I]R93274.

reagent grade obtained from conventional sources and were used without further purification.

Preparative and analytical high pressure liquid chromatography (HPLC) was carried out with a Spectra Physics 8800 ternary HPLC pump (San Jose, CA, USA), Spectra Physics 200 UV detector (at 275 nm), and a Canberra series 20 multichannel gamma detector (Canberra Industries, Meriden, CT, USA) using a 4 μ Novapak C-18 3.9 × 250 mm stainless steel column (Waters Associates, Milford, MA, USA) and a mobile phase of $CH_3OH/H_2O/(C_2H_5)_3N$ (66:32:0.1) at a flow rate of 0.7 ml/min. Retention time of the precursor (**1**) and the iodinated product (**2**) under these conditions was 11 and 32 min, respectively. Plasma analysis was carried out using an 8 mm Radial-Pak cartridge with radial compression module (Waters Associates, Milford, MA, USA), using a mobile phase of $CH_3OH/H_2O/(C_2H_5)_3N$ (80:20:0.1) at a flow rate of 1 ml/min.

Radiolabeling was performed as follows: to the sodium [^{123}I]iodide 1 ml shipping vial was added, through the septum, using 0.5 ml insulin syringes (B-D, Lo-dose, U-100 28G1/2) and in the following order: 50 μg (0.122 μmol) of the precursor (**1**, R91150) in 50 μl methanol (sonicated for 3 min to dissolve), a volume of 0.5 M H_3PO_4 equal to 1/5 the volume of Na^{123}I/NaOH solution, rounded to the nearest 5 units, and 100 μl of freshly prepared 0.02 M peracetic acid (100 μl 32% CH_3CO_3H in 2.4 ml water). After 30 min at room temperature, 50 μl (0.5 mg) 10 mg/ml aqueous $NaHSO_3$ solution was added and the vial headspace was purged into charcoal with a stream of N_2 or Ar for 3–4 min. The whole reaction mixture was diluted with 200–400 μl mobile phase, and injected into the HPLC. The fraction eluting at the retention time of [^{123}I]R93274 was collected and transferred to a 50 ml pear shaped flask containing 100 μl (450 μg) 4.5 mg/ml L-ascorbic acid. The solvent was evaporated under reduced pressure and the residue was dissolved in 400 μl ethanol and diluted with 8 ml 0.9% NaCl. The final solution (approximately 5% ethanol and 0.2 mM ascorbic acid at a pH of 5–5.5) was filtered through a 0.2 μm membrane filter (Acrodisc-13, Gelman Sciences, Ann Arbor, MI, USA) into a sterile 10 ml serum vial or 10 ml syringe. The radiochemical purity was measured by HPLC immediately after preparation and again after storage at

room temperature for 20–24 h. Radiochemical yield was calculated by dividing the radioactivity in the final purified product, corrected for decay, by the amount of starting [^{123}I]NaI. Radioactivities were measured in a gamma ionization chamber (Capintec CRC-7, Montvale, NJ, USA) calibrated for each geometry and vessel configuration. Sterility was confirmed by lack of growth in two media: fluid thioglycollate at 35°C and soybean-casein digest at 25°C for 2 weeks (USP XXII 1990). Apyrogenicity was confirmed by the LAL test (Endosafe, Charleston, NC, USA).

2.2. SPECT protocol

SPECT scanning experiments ($n = 5$) were performed in 3 female baboons (referred to as baboons A, B and C) according to protocols approved by the local animal care committee. Three control experiments were performed to study the brain regional uptake of [^{123}I]R93274, and two displacement experiments were performed to investigate the specificity and selectivity of the in vivo binding of [^{123}I]R93274.

Baboons were anesthetized with 2.5% isoflurane as previously described (Laruelle et al., 1994b). [^{123}I]R93274 (336.7 ± 40.7 MBq) was administered i.v. over 30 s. Data were acquired with the CERASPECT camera (Digital Scintigraphics, Waltham, MA, USA). Scans of 10 min duration were acquired in the continuous mode for 360 min. For the control experiments ($n = 3$, one in each baboon), an indwelling catheter was inserted in the femoral artery. Arterial blood samples were collected to study the metabolism of the tracer in plasma and to provide an input function for kinetic modeling of brain regional radioactivity uptake. Samples were obtained every 10 s for the first 2 min with a peristaltic pump (Harvard 2501-001, South Natick, MA, USA) and manually at 3, 4, 6, 8, 10, 12, 16, 20 and 30 min, and every 30 min thereafter.

In one displacement experiment, a receptor saturating dose of the 5-HT$_{2A}$ antagonist ketanserin (5 mg/kg i.v.) was injected at 150 min to investigate the specific nature of the regional uptake. In another experiment, the selectivity of [^{123}I]R93274 in vivo binding to 5-HT$_{2A}$ receptors relative to D$_2$ receptors was tested with an injection of the specific D$_2$ receptor antagonist raclopride (0.2 mg/kg i.v.) at 150 min. This dose of raclopride has been shown to displace completely the D$_2$ radiotracer 123-iodine-iodobenzofuran ([^{123}I]IBF) from the baboon striatum (Laruelle et al., 1994a).

2.3. Arterial plasma analysis

Metabolite analyses were carried out as previously described (Baldwin et al., 1993). Briefly, plasma was extracted with ethyl acetate and samples were analyzed by HPLC. Control samples (whole blood), incubated with [^{123}I]R93274 and preserved in the same conditions as the experimental samples (18–22 h at 4°C), were used to calculate the recovery and to verify stability of the compound in blood under these storage conditions. Plasma protein binding was measured by ultrafiltration (Gandelman et al., 1994) with membranes having a 30 000 molecular weight cut-off (Centrifree No. 4104, Amicon, Danvers, MA, USA).

For single bolus experiments, the concentrations in plasma over time of the free, metabolite-corrected tracer were fit to a sum of three exponentials:

$$f_1 C_1(t) = f_1 C_0 \sum_{i=1}^{3} a_i e^{-\lambda_i t} \quad (1)$$

where C_1 (MBq/l) is the metabolite-corrected arterial plasma concentration, f_1 (unitless) is the free fraction of the parent compound in the plasma, C_0 (MBq/l) is the peak plasma concentration, a_i (unitless) is the relative zero-time intercept for each exponential and λ_i (min^{-1}) is the elimination rate constant associated with each exponential. The half-life ($t_{0.5}$) of each exponential term was calculated as $\ln 2/\lambda_i$. The plasma clearance (C_l, l h^{-1}) was calculated as the ratio of the dose (MBq) to the total area under the curve of the free tracer time-activity curve (MBq h l^{-1}).

2.4. Image analysis

Images were reconstructed, attenuation corrected and reoriented as previously described (Laruelle et al., 1994b). Detected radioactivity (cpm) was converted to MBq using a calibration factor of 15 892 cpm/MBq, measured with an ^{123}I distributed source (Laruelle et al., 1994b). Total brain uptake was calculated by summing the intracerebral radioactivity from each brain slice, and was expressed as a percentage of the injected dose. Region of interest analyses were performed in reference to a baboon brain atlas (Riche et al., 1988) and to one MRI scan obtained in baboon A. The four images with highest cortical radioactivity were identified and summed. Occipital and temporal regions of interest were positioned on the resulting image. Frontal region of interest was positioned on the sum of three slices with highest frontal radioactivity. Two images corresponding to the striatal level were added for the striatal region of interest. Two images corresponding to the level of the cerebellum were summed for the cerebellar region of interest. The sizes of the regions of interest were as follows: occipital, 930 mm^2; temporal, 985 mm^2; frontal, 321 mm^2; striatum, 276 mm^2; cerebellum, 930 mm^2. Regional time-radioactivity curves were decay corrected to time of injection. Regional uptake was expressed in percentage injected dose per liter of brain tissue (%ID/l).

2.5. Quantitative analyses

A three-compartment model (Fig. 2) was used to analyze the time-radioactivity curves in the regions with de-

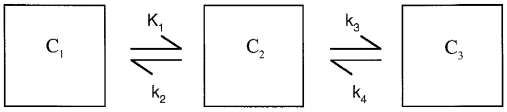

Fig. 2. Compartmental model used in this study. The model included the arterial plasma compartment (C_a), the intracerebral free and nonspecifically bound compartment (nondisplaceable compartment, C_2), and the specifically bound compartment (C_3). K_1 and k_2 measure the rate of transfer of the tracer across the blood-brain barrier, while k_3 and k_4 measure the rate of association and dissociation to and from the receptor compartment.

tectable specific binding (i.e., regions in which radioactivity was displaceable by ketanserin). This model included the arterial plasma compartment (C_1), the intracerebral free and nonspecifically bound compartment (nondisplaceable compartment, C_2), and the specifically bound compartment (C_3). The metabolite-corrected total arterial plasma concentration (C_1, free plus protein bound) was used as input function for derivation of the rate constants, and the regional volumes of distribution were divided by f_1 to correct for the presence of plasma protein binding (Eq. (2)). The cerebellum, a region with negligible density of 5-HT_{2A} receptors (Schotte et al., 1983), was used to define the nondisplaceable compartment. Fitting the data of the cerebellar region required a three-compartment model that included the arterial plasma compartment (C_a), the intracerebral free and rapidly equilibrating nonspecifically bound compartment (C_{2A}), and the slowly equilibrating nonspecifically bound compartment (C_{2B}).

Kinetic parameters were derived by nonlinear regression using a Levenberg-Marquart least squares minimization procedure (Levenberg, 1944) implemented in MATLAB (The Math Works, South Natick, MA, USA) as previously described (Laruelle et al., 1994b). In regions with specific binding, the distribution volume of the receptor compartment is the binding potential (BP, ml g^{-1}), equal to the product of the receptor density (B_{max}, nM or pmol/g brain tissue) and affinity ($1/K_d$, nM^{-1} or ml plasma per pmol). BP was calculated according to:

$$BP = \frac{K_1 k_3}{k_2 k_4 f_1} \quad (2)$$

In these regions, the value of the nondisplaceable volume of distribution was constrained to the value of the cerebellar volume of distribution (Laruelle et al., 1994a). The specific to nonspecific partition coefficient (V_3''), corresponding to the ratio of BP to the nondisplaceable distribution volume (V_2) was calculated as:

$$V_3'' = \frac{BP}{V_2} = \frac{k_3}{k_4} \quad (3)$$

The cerebellar total volume of distribution (V_2) was calculated as:

$$V_2 = V_{2A} + V_{2B} = \frac{K_1(1 + k_5/k_6)}{k_2 f_1} \quad (4)$$

We also performed a graphical analysis according to the method of Logan et al. (1990). In this method, the ratio of the integral of the input function from time 0 to time t to the regional radioactivity at time t is plotted against the ratio of the integral of regional radioactivity from time 0 to time t to the regional radioactivity at time t. This method allows for derivation of the regional distribution volumes without any assumptions about the number and configuration of the compartments. The only requirement for this method is the reversibility of radioactivity uptake. If the uptake is reversible, the plot will be linear, and its slope is the distribution volume. Integrations were performed numerically using a recursive Simpson's rule.

3. Results

3.1. Radiolabeling

The yield of the radiolabeling procedure was 61 ± 11% ($n = 5$, with this and subsequent values expressed as mean ± S.D.). The radiolabeled product was stable for at least 24 h at room temperature in normal saline, containing about 5% ethanol and 0.2 mM ascorbic acid; radiochemical purity was 98.6 ± 1% immediately after preparation and 95.6 ± 4% measured 20–24 h later. The specific activity was higher than 1 850 000 MBq/mmol.

3.2. Regional brain uptake

Total brain radioactivity peaked at 20–30 min at 1.06 ± 0.25% ID. Regional radioactivity uptake was examined in the occipital, temporal, striatal and cerebellar regions (Figs. 3 and 4A). In the cerebellum, peak radioactivity (4.8% ID/l) was recorded on the first image (0–10 min), and decreased thereafter at a rate of 22 ± 4% of peak value per h. Peak regional radioactivity was recorded later in the other regions (at 27 ± 11, 30 ± 16 and 21 ± 22 min in the occipital, temporal and striatal regions, respectively). At 30 min, regional radioactivity was 6.4 ± 0.7, 5.8 ± 0.7 and 4.9 ± 0.1% ID/l in the occipital, temporal and striatal regions, respectively. Following peak uptake, regional radioactivity declined at a rate of 18 ± 2, 18 ± 3 and 17 ± 5% of regional peak value per h in the occipital, temporal and striatal regions, respectively. High uptake was observed at the level of the eyes and orbital perioccular region (3.4 ± 0.4% ID/l). Because of the proximity of this area to the frontal cortex in baboons, the radioactivity in the frontal region of interest was contaminated by radioactivity from the eyes, which precluded accurate measurement of frontal radioactivity. The region of interest to cerebellum ratio progressively increased and reached a stable plateau at approximately 150 min at values of 1.49 ± 0.15, 1.42 ± 0.16 and 1.27 ± 0.06 in the occipital, temporal and striatal regions, respectively.

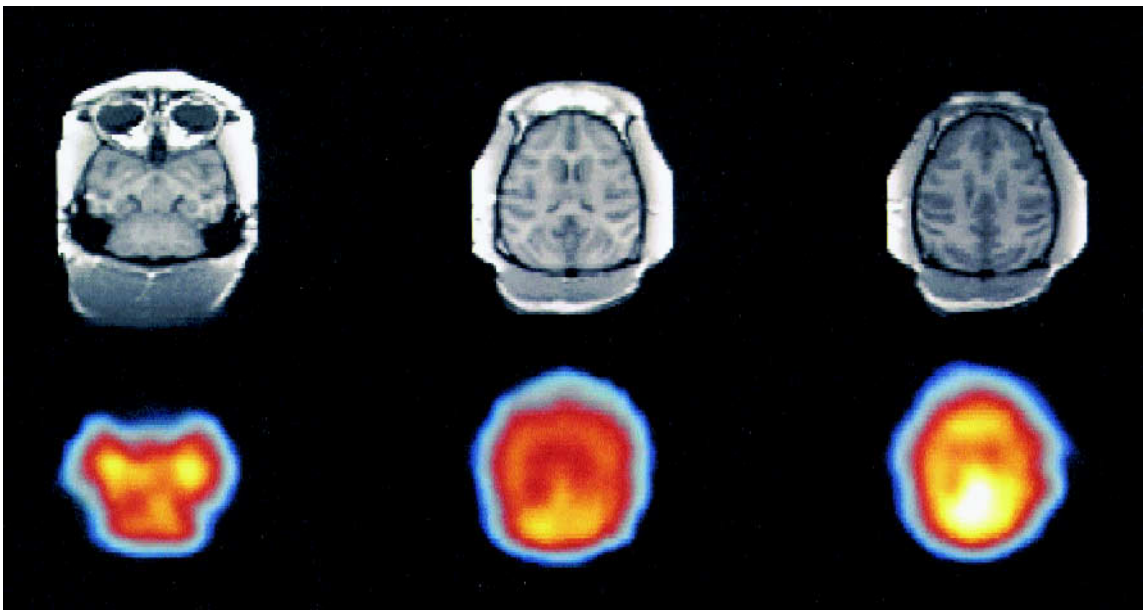

Fig. 3. [^{123}I]R93274 activity distribution at 30 min post injection (388.5 MBq) in the baboon brain (lower row) and corresponding MRI slices acquired in the same animal (upper row). The left column corresponds to the level of the cerebellum, midbrain and temporal poles. The middle column represents the level of the striatum. The right column corresponds to cerebral cortex.

3.3. Regional specificity

Injection of ketanserin (5 mg/kg) at 150 min post injection of the radiotracer resulted in a rapid displacement of radioactivity in the cortical and striatal regions to the level observed in the cerebellum (Fig. 4B). In contrast, ketanserin injection did not affect radioactivity in the cerebellum. Periorbital radioactivity uptake was not affected by ketanserin injection, which supports the hypothesis that this radioactivity corresponds to accumulation of radiolabelled metabolites. Raclopride injection (0.2 mg/kg) did not affect radioactivity uptake in any of the regions examined, including the striatum.

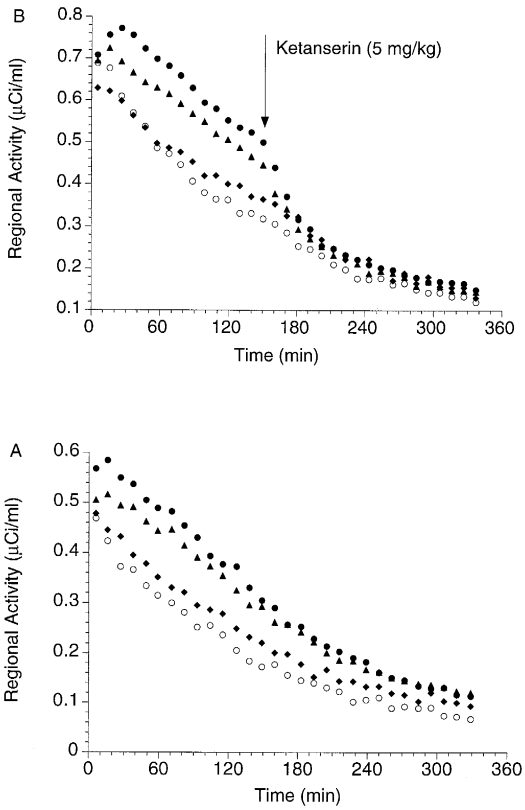

Fig. 4. Activities in occipital (●), temporal (▲), striatal (◆) and cerebellar (○) regions, following injection of 296.0 MBq [^{123}I]R93274 in baboon B. (A) Control experiment. (B) Displacement with ketanserin.

3.4. Arterial plasma analysis

The major metabolite was a polar, non-extractable fraction, which increased to $>50\%$ of the plasma radioactivity by 60 to 90 min (Fig. 5A). An extractable metabolite, less lipophilic than R93274 on HPLC, was also observed, and contributed to $<20\%$ of plasma radioactivity by 360 min ($n=6$). Thus, the contribution of the parent compound to the plasma radioactivity decreased rapidly over the first 2 h. At 120 min, the parent compound fraction was $24\pm10\%$ of the total radioactivity.

The concentration of the free parent tracer over time was fitted to a sum of three exponentials (Fig. 5B). Plasma clearance expressed relative to the total radiotracer (i.e., free plus protein bound) was 28.3 ± 11.9 l/min. Terminal half-lives were 0.60 ± 0.08, 18 ± 8 and 185 ± 32 min. Plasma free fraction of the parent compound (f_1) was $2.9\pm1.6\%$ of plasma parent compound concentration.

3.5. Quantitative analysis

Kinetic modeling of the cerebellar time-radioactivity curves with a three-compartment model provided a signifi-

Table 1
Compartmental analysis of the cerebellum uptake

Expt.	Baboon	K_1 (ml g^{-1} min^{-1})	k_2 (min^{-1})	k_5 (min^{-1})	k_6 (min^{-1})	V_2 (ml g^{-1})
1	A	0.0925	0.0434	0.0361	0.0217	196
2	B	0.1321	0.0495	0.0350	0.0282	206
3	C	0.1349	0.0508	0.0199	0.0138	224
Mean		0.1198	0.0479	0.0303	0.0212	209
±S.D.		0.0237	0.0039	0.0090	0.0072	14

Compartmental analysis of [^{123}I]R93274 uptake kinetics in the cerebellum. K_1 and k_2 are the rate constants for the transfer across the blood-brain barrier, k_5 and k_6 are the rate constants for transfer to and from the slowly equilibrating nonspecific compartment respectively. V_2 is the total cerebellar volume of distribution.

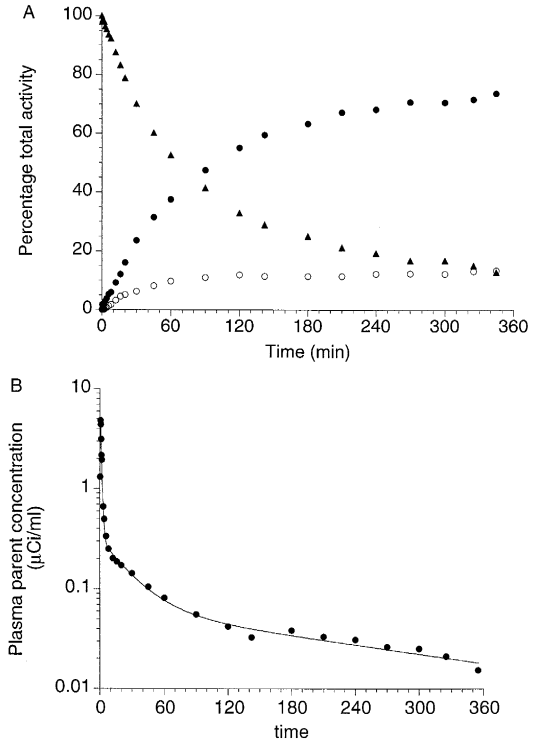

Fig. 5. Analysis of plasma activity after injection of 370 MBq [^{123}I]R93274 in baboon A. (A) Contribution of parent compound (▲), polar fraction (●) and lipophilic metabolite (○) to total plasma activity. (B) Parent compound concentration in plasma over time. The dots are the measured values and the line represents values fitted to a sum of three exponentials.

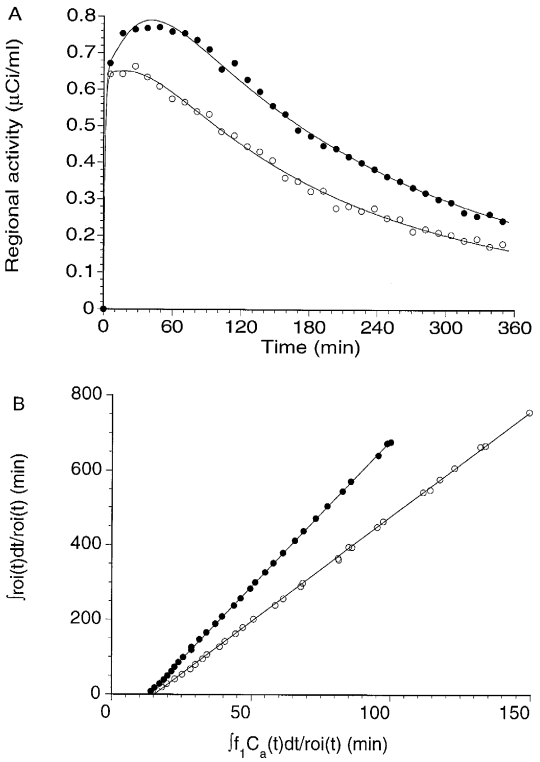

Fig. 6. Quantification of 5-HT$_{2A}$ receptors binding potential after injection of 370 MBq [^{123}I]R93274 in baboon A. Occipital (●) and cerebellar (○) activities were analyzed with both kinetic (panel A) and graphical (panel B) analyses. Both analyses yielded identical results (Table 2Table 3).

Table 2
Compartmental analysis of the occipital uptake

Expt.	Baboon	K_1 (ml g^{-1} min^{-1})	k_2 (min^{-1})	k_3 (min^{-1})	k_4 (min^{-1})	BP (ml) g^{-1}	V_3''
1	A	0.0821	0.0145	0.0123	0.0305	79	0.40
2	B	0.1189	0.0199	0.0064	0.0196	68	0.33
3	C	0.1368	0.0211	0.0081	0.0137	132	0.59
Mean		0.1126	0.0185	0.0089	0.0213	93	0.44
±S.D.		0.0279	0.0035	0.0030	0.0085	34	0.14

Compartmental analysis of [^{123}I]R93274 radioactivity uptake in the occipital. K_1 and k_2 are the rate constants of transfer across the blood-brain barrier; k_3 and k_4 are rate constants for transfer to and from the receptor compartment. The binding potential (BP, ml g^{-1}) is equal to the product of the receptor density (B_{max}, nM or pmol/g brain tissue) and affinity ($1/K_d$, nM^{-1} or ml plasma per pmol). The specific to nonspecific partition coefficient (V_3'') is the ratio of BP to the nondisplaceable distribution volume (V_2) and is equal to k_3/k_4 ratio. In this analysis, occipital V_2 was constrained to cerebellar V_2, by constraining the K_1/k_2 ratio to cerebellar V_2 f_1.

Table 3
Regional graphical analysis

Expt.	Baboon	Occipital pole		Temporal pole		Striatum	
		BP	V_3''	BP	V_3''	BP	V_3''
1	A	77	0.40	53	0.27	34	0.18
2	A	68	0.33	49	0.24	41	0.20
3	B	128	0.58	111	0.50	19	0.08
Mean		91	0.44	71	0.34	31	0.15
±S.D.		32	0.13	35	0.14	11	0.06

Results from graphical analysis of occipital, temporal and striatal uptake of [^{123}I]R93274 derived by the method of Logan et al. (1990). The binding potential (BP, ml g^{-1}) is equal to the product of the receptor density (B_{max}, nM or pmol/g brain tissue) and affinity ($1/K_d$, nM^{-1} or ml plasma per pmol) and was derived from the slope of the Logan plot of the region of interest. The specific to nonspecific partition coefficient (V_3'') is the ratio of BP to the nondisplaceable distribution volume (V_2) and was obtained as the ratio of the slope in the region of interest to the slope in the cerebellum.

cantly better fit than analysis with a two-compartment model (data not shown). The cerebellar volumes of distribution (V_2) derived from the three-compartment analysis were 196, 206, 224 ml/g in baboons A, B and C respectively (Table 1, Fig. 6A). These values were used in subsequent analyses to constrain the value of the nondisplaceable compartment in the other regions.

Kinetic analyses of occipital uptake were fitted to a three-compartment model (Table 2, Fig. 6A). Values for the transfer rate constants in the occipital were $K_1 = 0.1126 \pm 0.0279$; $k_2 = 0.0185 \pm 0.0035$; $k_3 = 0.0089 \pm 0.0030$; $k_4 = 0.0213 \pm 0.0085$. Identifiability of the rate constants was $1.8 \pm 0.3\%$ for K_1, $15 \pm 5\%$ for k_3 and $17 \pm 5\%$ for k_4. Identifiability of the BP (93 ± 34 ml/g) was $3.7 \pm 0.6\%$. Occipital V_3'' was 0.44 ± 0.14. Comparable results were obtained in the temporal region ($K_1 = 0.0963 \pm 0.0255$; $k_2 = 0.0158 \pm 0.0032$; $k_3 = 0.0072 \pm 0.0054$; $k_4 = 0.0224 \pm 0.0020$, BP $= 76 \pm 36$ ml/g, $V_3'' = 0.36 \pm 0.14$). The model did not converge in the striatum, presumably because of the very low value of the third compartment relative to the second compartment.

Results of the graphical analysis (occipital: BP $= 91 \pm 32$ ml/g; temporal: BP $= 71 \pm 35$ ml/g) were identical to results of the kinetic analysis. In the striatum, graphical analysis provided a BP of 31 ± 11 ml/g and a V_3'' of 0.15 ± 0.06 (Table 3, Fig. 6B).

4. Discussion

The feasibility of imaging 5-HT$_{2A}$ receptors with SPECT and [^{123}I]R93274 was evaluated in baboons. The tracer crossed the blood–brain barrier and concentrated in 5-HT$_{2A}$ receptor rich brain regions where it displayed specific, selective and reversible binding. However, brain uptake and target to background ratio were lower in baboons than in rats (Mertens et al., 1995).

Assuming a blood flow of 0.78 ml g^{-1} min^{-1} in the primate under anesthesia (Mintun et al., 1984), the K_1 value of 0.11 ml g^{-1} min^{-1} indicates a single pass extraction of 14% of the total parent compound. This low extraction may be due to the high binding to plasma protein (only 3% of the parent compound was free). The permeability-surface area product relative to the free compound was estimated as 4.7 ml g^{-1} min^{-1}, a value compatible with the high lipophilicity of the compound. Thus, the compound has a high permeability for the blood–brain barrier, but the extraction is limited by the high plasma protein binding.

Solvent extraction and HPLC analysis of plasma after i.v. administration of [^{123}I]R93274 in baboons revealed two metabolite fractions. The major fraction was polar and is not expected to cross the blood–brain barrier. This fraction was not analyzed further, so the number of polar metabolites was not determined. We also observed a smaller lipophilic fraction. We did not determine if this metabolite was present in the brain. Chemical analysis of brain tissue radioactivity would be needed to confirm the absence of [^{123}I]R93274 metabolites from the brain. However, given the small magnitude (< 20%) of this fraction, it is unlikely to interfere with the quantification of the receptors.

[^{123}I]R93274 was metabolized much more rapidly in baboons than in rats. At 3 h post injection, the parent compound radioactivity represented 95% of the plasma radioactivity in the rat (Mertens et al., 1995), as opposed to 25% in the baboon. Thus, in comparison with rats, baboons exhibited a higher rate of peripheral metabolism. For several SPECT neuroreceptor radiotracers, such as 123-iodine-methyl 3*b*-(4-iodophenyl) tropane-2*b*-carboxylate ([^{123}I]β-CIT) and [^{123}I]IBF, we observed a slower peripheral metabolism in humans compared to baboons (Laruelle et al., 1994a,c,d; Scanley et al., 1995). Thus, the fast metabolism of [^{123}I]R93274 in baboons is not necessarily predictive of a fast metabolism in humans.

Cerebellar radioactivity showed a rapid rate of washout. The rate of cerebellar washout was similar to the rate of elimination of the parent compound from the plasma. After 100 min post injection, the cerebellar radioactivity/plasma parent compound concentration ratio was stable, an observation which indirectly suggests that the lipophilic metabolites do not significantly cross the blood–brain barrier. The cerebellar radioactivity was not affected by ketanserin administration, which confirmed the nonspecific nature of the uptake, as expected from the reported absence of 5-HT$_{2A}$ receptors in this structure (Schotte et al., 1983). In the other regions examined, the radioactivity peaked later than in the cerebellum (at about 30 min). The injection of ketanserin reduced the uptake in these regions to the level observed in the cerebellum. This result demonstrates the presence of specific and reversible binding in these regions. 60 min post injection, the washout rate in the regions of interest was equal to that in cerebellum and in

plasma, meeting the definition of a transient equilibrium phase (see Carson et al., 1992).

The reversible nature of the binding allowed for both compartmental (kinetic) and noncompartmental (graphical) analyses, which yielded similar results. In the cortex, the binding potential ranged between 75 and 100 mg/ml. Assuming an in vivo K_d of 0.1 nM (a value measured in vitro in rat cortex Mertens et al., 1995), this BP is compatible with a B_{max} value of 7.5 to 10 nM. Given a brain protein concentration of 80 mg protein/g of brain tissue (Snyder et al., 1984) , the occipital B_{max} value of 10 nM corresponds to 125 fmol/mg protein, a value close to 5-HT_{2A} receptors B_{max} measured with [^{3}H]ketanserin in the human occipital cortex (136 ± 17 fmol/mg protein) (Laruelle et al., 1993). The markedly lower BP measured in the striatum (31 ± 11 ml/g) is in accordance with the lower density of 5-HT_{2A} receptors in the striatum compared to the cortex in primates. The density of 5-HT_{2A} receptors in the human basal ganglia is approximately a third of the density in the human cortex (Schotte et al., 1983; Hoyer et al., 1986).

The density of 5-HT_{2A} receptors is about three times higher in the rat cortex compared to primate cortex (Leysen et al., 1982; Luabeya et al., 1984). Thus, a lower target to background ratio in primates as opposed to rodents has been a common finding in the development of radiotracers to visualize 5-HT_{2A} receptors (Sadzot et al., 1995). For [^{123}I]R93274, a higher nonspecific binding also contributed to the lower cortical to cerebellar ratio observed in baboons (1.5) compared to rats (10). In baboons, the cerebellar volume of distribution relative to the total plasma parent compound concentration was 6.0 ± 0.4 ml/g, as compared to approximately 1.6 ml/g in the rat.

Because of its high selectivity for 5-HT_{2A} receptors, [^{123}I]R93274 compares favorably with [^{11}C]NMSP and [^{18}F]setoperone, both tracers with significant affinity for D_2 receptors (Wong et al., 1984; Blin et al., 1988, 1990). On the other hand, [^{123}I]R93274 is inferior to the PET tracer [^{18}F]altanserin which combines a good selectivity with a cortical to cerebellar ratio higher than [^{123}I]R93274 (2.5 versus 1.5). However, because of the widespread availability of SPECT compared to PET, further evaluation of [^{123}I]R93274 in humans is warranted.

Acknowledgements

The authors wish to acknowledge L. Pantages Torok and Melissa Madrak for excellent technical assistance, E.O. Smith, G. Wisniewski, M. Early for nuclear medicine technologist support.

References

Aghajanian, G.K., 1994, Serotonin and the action of LSD in the brain, Psychiatr. Ann. 24, 137.

Arora, R.C. and H.Y. Meltzer, 1989, Serotonergic measures in the brains of suicide victims: 5-HT_2 binding sites in the frontal cortex of suicide victims and control subjects, Am. J. Psychiatry 146, 730.

Arora, R.C. and H.Y. Meltzer, 1991, Serotonin$_2$ (5-HT_2) receptor binding in frontal cortex of schizophrenic patients, J. Neural Transm. 85, 19.

Baldwin, R.M., Y. Zea-Ponce, S.S. Zoghbi, M. Laruelle, M.S. Al-Tikriti, E.H. Sybriska, R.T. Malison, J.L. Neumeyer, R.A. Milius, S. Wang, M. Stabin, E.O. Smith, D.S. Charney, P.B. Hoffer and R.B. Innis, 1993, Evaluation of the monoamine uptake site ligand [^{123}I]methyl 3β-(4-iodophenyl)tropane-2β-carboxylate ([^{123}I]β-CIT) in nonhuman primates: pharmacokinetics, biodistribution and SPECT imaging coregistered with MRI, Nucl. Med. Biol. 20, 597.

Bennett, J.P., S.J. Enna, D.B. Bylund, J.C. Gillin, R.J. Wyatt and S.H. Snyder, 1979, Neurotransmitter receptors in frontal cortex of schizophrenics, Arch. Gen. Psychiatry 36, 927.

Berridge, M., D. Comar, C. Crouzel and J.C. Baron, 1983, ^{11}C-labeled ketanserin: a selective serotonin S_2 antagonist, J. Label. Compd. Radiopharm. 20, 73.

Blin, J., S. Pappata, M. Kijosawa, C. Crouzel and J.C. Baron, 1988, [^{18}F]Setoperone: a new high-affinity ligand for positron emission tomography study of the serotonin-2 receptors in baboon brain in vivo, Eur. J. Pharmacol. 147, 73.

Blin, J., G. Sette, M. Fiorelli, O. Bletry, J.L. Elghozi, C. Crouzel and J.C. Baron, 1990, A method for the in vivo investigation of the serotonergic 5-HT_2 receptors in the human cerebral cortex using positron emission tomography and ^{18}F-labeled setoperone, J. Neurochem. 54, 1744.

Blin, J., J.C. Baron, B. Dubois, C. Crouzel, M. Fiorelli, D. Attar-Levy, B. Pillon, D. Fournier, M. Vidailhet and Y. Agid, 1993, Loss of brain 5-HT_2 receptors in Alzheimer's disease. In vivo assessment with positron emission tomography and [^{18}F]setoperone, Brain 116, 497.

Carson, R.E., M.A. Channing, R.G. Blasberg, B.B. Dunn, R.M. Cohen, K.C. Rice and P. Herscovitch, 1992, Comparison of bolus and infusion methods for receptor quantification: application to [^{18}F]cyclofoxy and positron emission tomography, J. Cereb. Blood Flow Metab. 13, 24.

Cheetham, S.C., M.R. Crompton, C.L.E. Katona and R.W. Horton, 1988, Brain 5-HT_2 receptor binding sites in depressed suicide victims, Brain Res. 443, 272.

Crow, T.J., A.J. Cross, S.J. Cooper, J.F.W. Deakin, I.N. Ferrier, J.A. Johnson, M.H. Joseph, F. Owen, M. Poulter, R. Lofthouse, J.A.N. Corsellis, D.R. Chambers, G. Blessed, E.K. Perry and E.H. Perry, 1984, Neurotransmitter receptors and monoamine metabolites in the patients with Alzheimer-type dementia and depression, and suicides, Neuropharmacology 23, 1561.

Gandelman, M.S., R.M. Baldwin, S.S. Zoghbi, Y. Zea-Ponce and R.B. Innis, 1994, Evaluation of ultrafiltration for the free fraction determination of single photon emission computerized tomography (SPECT) radiotracers: β-CIT, IBF and iomazenil, J. Pharm. Sci. 83, 1014.

Gross-Isseroff, R., D. Salama, M. Israeli and A. Biegon, 1990, Autoradiographic analysis of [^{3}H]ketanserin binding in the human brain postmortem: effect of suicide, Brain Res. 507, 208.

Hoyer, D., A. Pazos, A. Probst and J.M. Palacios, 1986, Serotonin receptors in the human brain. II. Characterization and autoradiographic localization of 5-HT_C and 5-HT_2 recognition sites, Brain Res. 376, 97.

Joyce, J.N., A. Shane, N. Lexow, A. Winokur, M.F. Casanova and J.E. Kleinman, 1993, Serotonin uptake sites and serotonin receptors are altered in the limbic system of schizophrenics, Neuropsychopharmacology 8, 315.

Laruelle, M., A. Abi-Dargham, M.F. Casanova, R. Toti, D.R. Weinberger and J.E. Kleinman, 1993, Selective abnormalities of prefrontal serotonergic receptors in schizophrenia: a postmortem study, Arch. Gen. Psychiatry 50, 810.

Laruelle, M., M.S. Al-Tikriti, Y. Zea-Ponce, S.S. Zoghbi, R.M. Baldwin, D.S. Charney, P.B. Hoffer, H.F. Kung and R.B. Innis, 1994a, In vivo quantification of dopamine D_2 receptors parameters in nonhuman

primates with [^{123}I]iodobenzofuran and single photon emission computerized tomography, Eur. J. Pharmacol. 263, 39.

Laruelle, M., R.M. Baldwin, Z. Rattner, M.S. Al-Tikriti, Y. Zea-Ponce, S.S. Zoghbi, D.S. Charney, J.C. Price, J.J. Frost, P.B. Hoffer and R.B. Innis, 1994b, SPECT quantification of [^{123}I]iomazenil binding to benzodiazepine receptors in nonhuman primates. I. Kinetic modeling of single bolus experiments, J. Cereb. Blood Flow Metab. 14, 439.

Laruelle, M., C. Van Dyck, A. Abi-Dargham, Y. Zea-Ponce, S.S. Zoghbi, D.S. Charney, R.M. Baldwin, P.B. Hoffer, H.F. Kung and R.B. Innis, 1994c, Compartmental modeling of iodine-123-iodobenzofuran binding to dopamine D_2 receptors in healthy subjects, J. Nucl. Med. 35, 743.

Laruelle, M., E. Wallace, J.P. Seibyl, R.M. Baldwin, Y. Zea-Ponce, S.S. Zoghbi, J.L. Neumeyer, D.S. Charney, P.B. Hoffer and R.B. Innis, 1994d, Graphical, kinetic and equilibrium analysis of [^{123}I]β-CIT in vivo binding to dopamine transporters in healthy subjects, J. Cereb. Blood Flow Metab. 14, 982.

Lemaire, C., R. Cantineau, M. Guillaume, A. Plenevaux and L. Christiaens, 1991, Fluorine-18-altanserin: a radioligand for the study of serotonin receptors with PET: radiolabeling and in vivo biologic behavior in rats, J. Nucl. Med. 32, 2266.

Levenberg, K., 1944, A method for the solution of certain problems in least squares, Q. Appl. Math. 2, 164.

Leysen, J.E., J.E. Niemeggers, J.M. Van Nueten and P.M. Laduron, 1982, [^{3}H]Ketanserin (R 41 468), a selective ^{3}H-ligand for serotonin-2 receptor binding sites: binding properties, brain distribution and functional role, Mol. Pharmacol. 21, 301.

Leysen, J.E., P.M.F. Janssen, A.A.H.P. Megens and A. Schotte, 1994, Risperidone: a novel antipsychotic with balanced serotonin-dopamine antagonism, receptor occupancy profile, and pharmacologic activity, J. Clin. Psychiatry 55 (Suppl.), 5.

Logan, J., J. Fowler, N.D. Volkow, A.P. Wolf, S.L. Dewey, D.J. Schlyer, R.R. MacGregor, R. Hitzermann, B. Bendriem, S.J. Gatley and D.R. Christman, 1990, Graphical analysis of reversible radioligand binding from time-activity measurements applied to [*N*-^{11}C-methyl]-(−)-cocaine PET studies in human subjects, J. Cereb. Blood Flow Metab. 10, 740.

Lowther, S., F. De Paermentire, R. Crompton, C.L.E. Katona and R.W. Horton, 1994, Brain 5-HT_2 receptors in suicide victims: violence of death, depression and effects of antidepressant treatment, Brain Res. 642, 281.

Luabeya, M.K., J.M. Maloteaux and P. Laduron, 1984, Regional and cortical distribution of serotonin S_2, benzodiazepine, muscarinic and dopamine D_2 receptors in human brain, J. Neurochem. 43, 1068.

Mann, J.J., M. Stanley, P.A. McBride and B.S. McEwen, 1986, Increased serotonin$_2$ and beta receptor in the frontal cortices of suicide victims, Arch. Gen. Psychiatry 43, 954.

Mayberg, H.S., R.G. Robinson, D.F. Wong, R. Parikh, P. Bolduc, S.E. Starkstein, T. Price, R.F. Dannals, J.M. Links, A.A. Wilson et al., 1988, PET imaging of cortical S_2 serotonin receptors after stroke: lateralized changes and relationship to depression, Am. J. Psychiatry 145, 937.

McKeith, I.G., E.F. Marshall, I.N. Ferrier, M.M. Armstrong, W.N. Kennedy, R.H. Perry, E.K. Perry and D. Eccleston, 1987, 5-HT receptor binding in post-mortem brains from patients with affective disorder, J. Affect. Disord. 13, 67.

Meltzer, H., 1989, Clinical studies on the mechanism of action of clozapine: the dopamine-serotonin hypothesis of schizophrenia, Psychopharmacology 99, S18.

Mertens, J., D. Terriere, V. Sipido, W. Gommeren, P.M.F. Janssen and J.E. Leysen, 1995, Radiosynthesis of a new radioiodinated ligand for serotonin-5HT_2-receptors, a promising tracer for gamma-emission tomography, J. Label. Compd. Radiopharm. 34, 795.

Mintun, M.A., M.E. Raichle, M.R. Kilbourn, G.F. Wooten and M.J. Welch, 1984, A quantitative model for the in vivo assessment of drug binding sites with positron emission tomography, Ann. Neurol. 15, 217.

Mita, T., S. Hanada, N. Nishino, T. Kuno, H. Nakai, T. Yamadori, Y. Mizoi and C. Tanaka, 1986, Decreased serotonin S_2 and increased dopamine D_2 receptors in chronic schizophrenics, Biol. Psychiatry 21, 1407.

Moerlein, S. and J.S. Perlmutter, 1991, Central serotonergic S_2 binding in *Papio anubis* measured in vivo with *N-o*-[^{18}F]fluoroethylketanserin and PET, Neurosci. Lett. 123, 23.

Nyberg, S., L. Farde, L. Eriksson, C. Halldin and B. Eriksson, 1993, 5-HT_2 and D_2 dopamine receptor occupancy in the living human brain. A PET study with risperidone, Psychopharmacology 110, 265.

Perry, E.K., R.H. Perry, J.M. Candy, A.F. Fairbairn, G. Blessed, D.J. Dick and B.E. Tomlinson, 1984, Cortical serotonin-S_2 receptor binding abnormalities in patients with Alzheimer's disease: comparisons with Parkinson's disease, Neurosci. Lett. 51, 353.

Reynolds, G.P., L. Arnold, M.N. Rossor, L.L. Iversen, C.Q. Mountjoy and M. Roth, 1984, Reduced binding of [^{3}H]ketanserin to cortical 5-HT_2 receptors in senile dementia of the Alzheimer type, Neurosci. Lett. 44, 47.

Riche, D., P. Hantraye, B. Guibert, R. Naquet, C. Loch'h and M. Mazière, 1988, Anatomical atlas of the baboon's brain in the orbitomeatal plane used in experimental positron emission tomography, Brain Res. Bull. 20, 283.

Sadzot, B., C. Lemaire, P. Maquet, E. Salmon, A. Plenevaux, C. Degueldre, J.P. Hermanne, M. Guillaume, R. Cantineau, D. Comar et al., 1995, Serotonin 5HT_2 receptor imaging in the human brain using positron emission tomography and a new radioligand, [^{18}F]altanserin: results in young normal controls, J. Cereb. Blood Flow Metab. 15, 787.

Scanley, B.E., M.S. Al-Tikriti, M.S. Gandelman, M. Laruelle, Y. Zea-Ponce, R.M. Baldwin, S.S. Zoghbi, P.B. Hoffer, D.S. Charney, S. Wang, J.L. Neumeyer and R.B. Innis, 1995, Comparison of [^{123}I]β-CIT and [^{123}I]IPCIT as single-photon emission tomography radiotracers for the dopamine transporter in nonhuman primates, Eur. J. Nucl. Med. 22, 4.

Schotte, A., J.M. Maloteaux and P.M. Laduron, 1983, Characterization and regional distribution of serotonin S_2-receptors in human brain, Brain Res. 276, 231.

Snyder, W.S., M.I. Cook, L.R. Karhausen, E.S. Nasset, G.P. Howells and I.H. Tipton, 1984, Central nervous system, in: Report of the Task Group on Reference Man (Pergamon Press, New York, NY) p. 281.

Stanley, M. and J.J. Mann, 1983, Increased serotonin-2 binding sites in frontal cortex of suicide victims, Lancet 2, 214.

Whitaker, P.M., T.J. Crow and I.N. Ferrier, 1981, Tritiated LSD binding in frontal cortex in schizophrenia, Arch. Gen. Psychiatry 38, 278.

Wong, D.F., H.N. Wagner, R.F. Dannals, J.M. Links, J.J. Frost, H.T. Ravert, A.A. Wilson, A.E. Rosenbaum, A. Gjedde, K.H. Douglass, J.D. Petronis, M.F. Folstein, J.K.T. Toung, H.D. Burns and M.J. Kuhar, 1984, Effects of age on dopamine and serotonin receptors measured by positron emission tomography in the living brain, Science 226, 1393.

Wong, D.F., J.R. Lever, P.R. Hartig, R.F. Dannals, V. Villemagne, B.J. Hoffman, A.A. Wilson, H.T. Ravert, J.M. Links, U. Scheffel and H.N. Wagner, 1987, Localization of serotonin 5HT_2 receptors in living human brain by positron emisssion tomography using *N*1-[^{11}C]-methyl)-2-Br-LSD, Synapse 1, 393.

Yates, M., A. Leake, J. Candy, A. Fairbairn, I. McKeith and I. Ferrier, 1990, 5HT_2 receptors changes in major depression, Biol. Psychiatry 27, 489.